Volume 16
Number 8
28 February 2025
Pages 3349–3760

Chemical Science

rsc.li/chemical-science

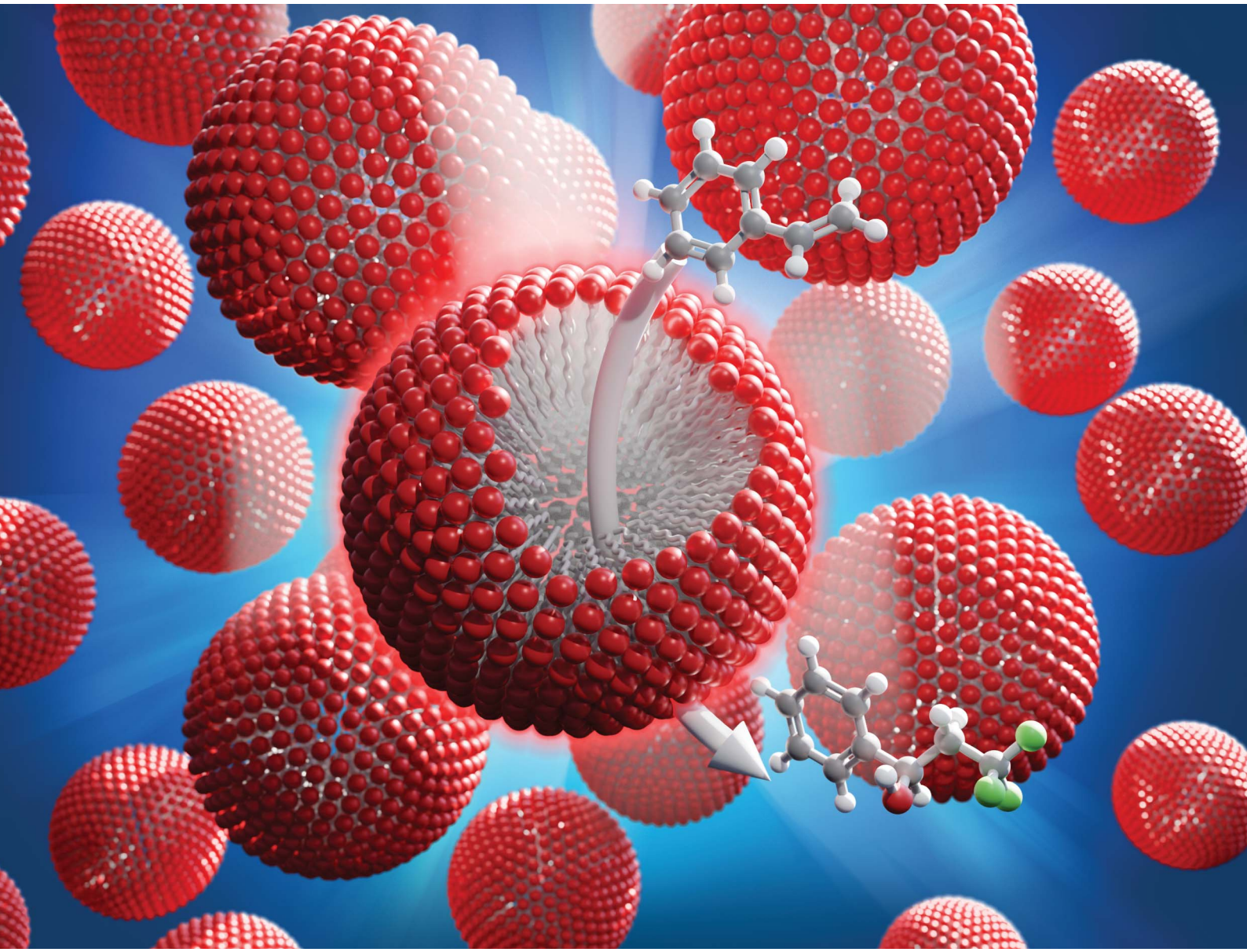

ISSN 2041-6539

ROYAL SOCIETY OF CHEMISTRY

EDGE ARTICLE
Angel A. Martí *et al.*
Supramolecular self-assembly of metal complex surfactants (MeCS) into micellar nanoscale reactors in aqueous solution

15 YEARS ANNIVERSARY

Chemical Science

ROYAL SOCIETY OF CHEMISTRY

EDGE ARTICLE

View Article Online
View Journal | View Issue

Cite this: *Chem. Sci.*, 2025, **16**, 3440

All publication charges for this article have been paid for by the Royal Society of Chemistry

Received 11th November 2024
Accepted 16th December 2024

DOI: 10.1039/d4sc07623k

rsc.li/chemical-science

Supramolecular self-assembly of metal complex surfactants (MeCS) into micellar nanoscale reactors in aqueous solution†

Ying Chen, [a] Asia Matatyaho Ya'akobi, [b] Thao Vy Nguyen,[c] Shih-Chieh Kao,[a] Julian G. West, [a] Sibani Lisa Biswal, [c] Yeshayahu Talmon [b] and Angel A. Martí *[ad]

Surfactants are amphiphilic molecules that can form micellar structures with a hydrophobic core and a hydrophilic corona in water. In this work, we combine the remarkable properties of photoactive metal complexes with the supramolecular organization of surfactants to create photoactive vessels that support photocatalytic processes in aqueous media, even for starting materials that are insoluble in water. Herein, we report a library of photoactive metal complex surfactants (MeCSs) and their photophysical and photochemical properties. These properties are modulated by the length of an alkyl chain attached to the polypyridyl ligand of the metal complex. Finally, an alkene hydroxytrifluoromethylation photocatalytic reaction was demonstrated in aqueous solution, suggesting the usefulness of metal complex surfactants for the development of green aqueous photoreactions.

Introduction

Metal polypyridyl complexes have been used for many applications over the past century due to their excellent photoredox properties.[1–6] In particular, metal complexes can form stable, long-lived excited states upon photoexcitation, which facilitates the interactions with substrates during the excited state, enabling a variety of novel reactions under mild conditions.[1] For example, the use of tris(2,2′-bipyridine)ruthenium(II) ($[Ru(bpy)_3]^{2+}$) as a visible light photoredox catalyst for organic synthesis has been well studied.[4,7–12] However, most of these reactions are diffusion-controlled and typically performed in organic solvents due to solubility constraints of substrates and catalysts. Recent efforts have focused on the use of aqueous media to improve sustainability in organic synthesis. Nevertheless, the use of water as a medium for visible-light photocatalytic transformations has not been thoroughly explored, partly due to the solubility challenges of reactants.[13]

Over the past several decades, many surfactants with novel properties have been designed and synthesized for various applications.[14–18] Previously, we have shown that fluorescent surfactants, such as rhodamine-B and eosin-Y attached to aliphatic chains, can self-assemble into micelles.[17] These fluorescent surfactants were used for applications including cellular imaging, labeling, and diffusion studies of nanotubes and nanosheets.[19,20] Recently, amphiphilic metal complexes with hydrophobic moieties on their ligands have been studied for their stability in both ground and photoexcited states and their rich redox/photophysical properties.[21–25] Many of these studies have primarily focused on double or multi-chain metal complex surfactants, where the number of chains attached to the surfactant leads to the formation of vesicles of micrometer dimensions.[26–33] Pioneer work by the Lipshitz group in 2018 showed the use of amphiphilic metal complexes in photoredox transformations in water, where they use a double-chain iridium complex (attached to a modified CoQ_{10} group with an aliphatic chain of 50 carbon atoms and a PEG group) forming micelles around 50 nm in diameter for the sulfonation of alkanes and enol acetates.[34]

In this work, we used a simple esterification reaction to synthesize a single-chain metal complex surfactant (MeCS) with a ruthenium polypyridyl cationic head and aliphatic groups of different lengths (6, 10, 12, and 16 carbons; Scheme 1). These ruthenium MeCSs were thoroughly characterized, allowing us to correlate their photophysical properties (photoluminescence quantum yield and lifetime) and their critical micelle concentration (CMC) with the chain length. Optimized ruthenium MeCSs were used as a proof-of-concept for the photocatalytic hydroxytrifluoromethylation of aryl alkenes in aqueous solution. To the best of our knowledge, no single study has comprehensively

[a]Department of Chemistry, Rice University, Houston, Texas, 77005, USA. E-mail: amarti@rice.edu

[b]Department of Chemical Engineering, The Russell Berrie Nanotechnology Institute, Technion-Israel Institute of Technology, Haifa 3200003, Israel

[c]Department of Chemical and Biomolecular Engineering, Rice University, Houston, TX 77005, USA

[d]Department of Materials Science & Nanoengineering, Department of Bioengineering, Rice University, Houston, TX. 77005, USA

† Electronic supplementary information (ESI) available. See DOI: https://doi.org/10.1039/d4sc07623k

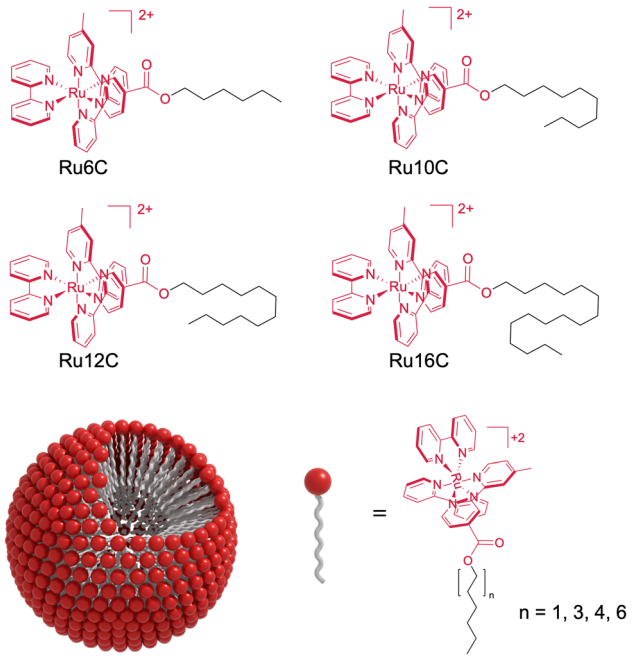

Scheme 1 Structure of Ru(II) surfactants (top) and assembled micelle (bottom).

examined single-chain ruthenium amphiphiles, including their synthesis, spectroscopic properties, self-aggregation behavior, and photocatalytic applications in aqueous media. This work fills that gap by providing a detailed investigation of these amphiphiles, highlighting their nanoscale micelle formation (5–6 nm), simple synthesis, and exceptional photophysical properties. In the context of sustainable chemistry, MeCSs offer a promising platform for photocatalytic reactions in water, enabling sustainable applications in pharmaceuticals and materials science.

Results and discussion

The minimum concentration needed for surfactant monomers to assemble into micelles is called the CMC.[35] Once the micelles form, their hydrophobic cores behave as nanoscale lipophilic vessels, which is convenient for photophysical and photocatalytic applications. Here, the pendant drop method was used to determine the interfacial tension of aqueous solutions with different surfactant concentrations.[36] Increasing the surfactant concentration decreases the surface tension of a pendant drop due to the migration of the surfactant to the interface between the drop and air (Fig. 1a). Once the CMC is reached, the concentration of monomers at the interface (and the surface tension) reaches a steady state, and any additional surfactant assembles into micelles (Fig. 1b).[37] Interestingly, a decrease in the CMC is observed as the alkyl chain length increases (Fig. 1c and S1†). The increase in alkyl chain length causes the surfactant to become more hydrophobic, promoting the aggregation of MeCSs into micelles at lower concentrations and decreasing the CMC.[38]

Cryo-TEM studies show that ruthenium surfactant Ru16C forms spheroidal micelles in aqueous solution (Fig. 2a). Likewise, round spheroidal structures are observed for a 4 mM solution of Ru12C, which is above the CMC. Images for Ru12C are shown in Fig. S3.† The micelles are readily visible given the contrast of the ruthenium complex in the cryo-TEM and have a mean diameter of 5.9 and 5.5 nm for Ru12C and Ru16C, respectively (Fig. S4†). The average hydrodynamic diameter of Ru12C and Ru16C were also determined as 16.2 nm and 25.0 nm by using dynamic light scattering (DLS) (Fig. S5†). Mixed micelles with 20 mM cetrimonium bromide (CTAB) and 1 mM Ru16C can also be formed, as seen in Fig. 2b. Similarly to Ru16C, CTAB is a cationic surfactant with a trimethylammonium ionic head and an aliphatic tail of 16 carbon atoms, similar in structure to Ru16C. The interfacial tension of the mixture of Ru16C and CTAB with different dilutions was obtained (Fig. S2†). Here, only one CMC value was observed, which is consistent with the formation of mixed micelles containing CTAB and Ru16C.

The absorption and emission spectra, photoluminescence quantum yield, and luminescence lifetimes of MeCSs were investigated in aqueous solution and compared to $[Ru(bpy)_3]^{2+}$.[39–41] All photophysical experiments of pure MeCS in solution were performed in nitrogen-purged solutions to avoid quenching by molecular oxygen[42] and below their CMC to prevent potential self-quenching.[43,44] CTAB was added to study the effect of micelle formation on the MeCS properties. CTAB is

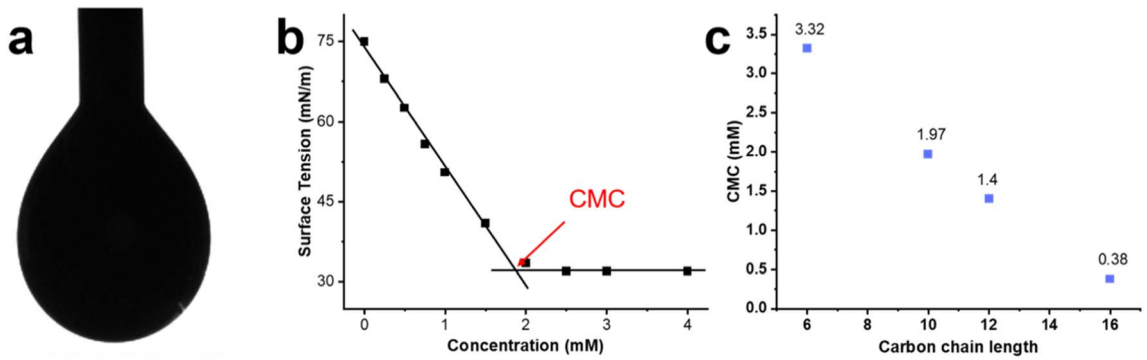

Fig. 1 CMC determination by the pendant drop method. (a) Example of the pendant drop image used to determine the surface tension of the different MeCS concentrations. (b) Surface tension for different concentrations of Ru10C (a ruthenium complex surfactant containing a decane aliphatic chain). (c) Trends in CMC for the four surfactants as a function of the number of carbons in the aliphatic chain.

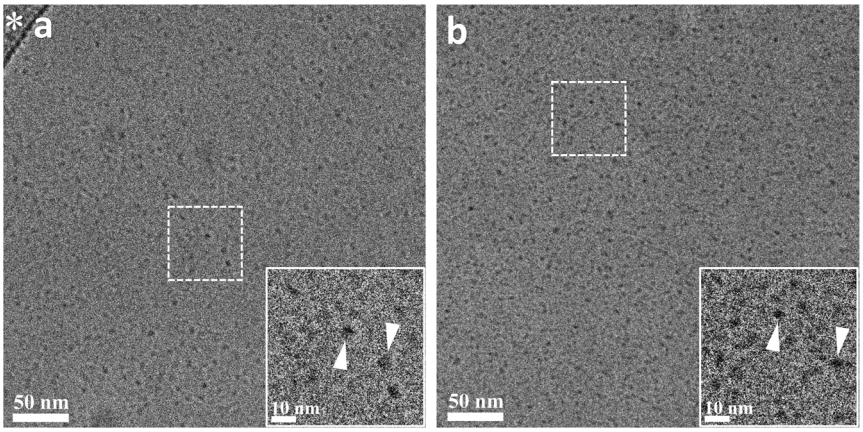

Fig. 2 Cryo-TEM micrographs of Ru16C and Ru16C-CTAB in water. (a) 4 mM Ru16C micellar solution, and (b) a solution of 1 mM Ru16C and 20 mM CTAB. Dashed squares mark the magnified areas shown in the insets. Arrowheads point to globular surfactant micelles. '*' denotes the perforated carbon film on the TEM grid that supports the vitrified solution.

optically transparent in the visible range and forms mixed micelles with MeCSs, allowing a low MeCS concentration in the micellar environment.

Spectroscopic studies show that ruthenium MeCSs present similar absorption spectra to that reported for $[Ru(bpy)_3]^{2+}$ with a broad metal-to-ligand charge transfer (MLCT) band around 460 nm.[39] Furthermore, it was also observed that the length of the alkyl chain did not change the shape of the photoluminescence spectra of the various MeCSs. The absorption and emission spectra of Ru16C are shown in Fig. S6.† Quantum yields for the different ruthenium MeCS are included in Table 1. As expected, the quantum yield for ruthenium MeCS in nitrogen-purged solutions is remarkably higher than in air and consistently increases with the number of carbon atoms in the aliphatic chain. Photoluminescence lifetime experiments also show an increase in the lifetime for all nitrogen-purged solutions (Table 1), but not a strong dependance with alkyl chain length. It is important to note that ruthenium MeCS in micelles does not seem to suffer from self-quenching. Actually, the quantum yield and photoluminescence lifetimes seem to be relatively independent of whether the ruthenium MeCS is monomeric or incorporated in CTAB micelles. This observation contrasts with ruthenium complexes with two alkyl chains in liposomes, where both the quantum yield and lifetimes are significantly reduced, indicating a strong deactivation of the excited state.[27] These contrasting behaviors might be related to the difference in size between micelles and liposomes, which will affect the packing and interaction of the ruthenium complexes in these environments. A more complete spectroscopic characterization of these systems would be necessary to clarify these observations.

In the last 10 years, groundbreaking research has shown the application of metallosurfactants in the production of solar fuels,[27,33,46,47] however, efforts to use metallosurfactants in aqueous photocatalytic transformations of organic products are less common.[34] Given their self-assembly, core hydrophobicity, and outstanding photophysical properties, we studied the use of MeCSs as nanoscale photoreactors for chemical reactions in aqueous solution. As a proof-of-concept, we studied the hydroxytrifluoromethylation of alkenes to evaluate the catalytic

Table 1 Photophysical properties of ruthenium surfactants in aqueous solution[a]

Sample	λ_{max} (nm)	λ_{max}^{em} (nm)	ϕ_{em}[b] (air)	ϕ_{em}[b] (N_2)	τ_{em}[c] (ns) (air)	τ_{em}[c] (ns) (N_2)
Ru6C	466	684	0.012	0.057	168.2 ± 0.5	484 ± 4[d]
Ru6C-CTAB				0.056		524 ± 4[d]
Ru10C	464	681	0.019	0.058	203.0 ± 0.6	516 ± 6[d]
Ru10C-CTAB				0.093		490 ± 5[d]
Ru12C	462	684	0.023	0.124	231.6 ± 0.6	532 ± 1
Ru12C-CTAB				0.097		546 ± 1
Ru16C	462	677	0.016	0.134	264.7 ± 0.6	539 ± 1
Ru16C-CTAB				0.149		494 ± 1

[a] The absorbance and emission spectra were obtained with ruthenium surfactant that was dissolved in water, and nitrogen-purged water at 298 K (λ_{ex} = 460 nm). [b] All the errors are less than 3%. [c] Unless otherwise indicated, the photoluminescence decays are monoexponential. [d] The luminescence decays are biexponential. The weighted mean lifetimes (τ_{em}) were calculated according to $\sum_{i=1}^{n}(f_i\tau_i)$, where f_i is the fractional contribution and τ_i is the decay time.[45]

efficiency of the ruthenium MeCSs, given the importance of trifluoromethylation of small molecules in the pharmaceutical[48,49] and agrochemical industries.[50]

In 2012, the Akita group reported the use of photoactive metal complexes as photoredox catalysts for the hydroxytrifluoromethylation of alkenes and further studies have now been reported.[51–54] However, these reactions were carried out in organic solvents to fully solubilize the substrates. Since ruthenium MeCSs have a ruthenium polypyridyl head group, as well as good water solubility, these photoactive micellar structures were used to initiate the desired hydroxytrifluoromethylation. Ru16C was chosen as a photocatalyst due to its lowest CMC and best photophysical properties (*e.g.*, τ_{em} and ϕ_{em}) among the other synthesized surfactants.

We set out to use styrene (1.1 equiv.) as the model substrate, Umemoto's reagent (**2a**, **2c**) and Togni's reagent (**2b**), trifluoromethyl thianthrenium triflate (TT-$CF_3^+OTf^-$, **2d**) as the CF_3 source, and 1 mol% of Ru16C as the photoredox catalyst in water (Table 2 and Fig. S7†). All these experiments confirmed the formation of 3,3,3-trifluoro-1-propan-1-ol (**3**) products. Umemoto's reagent affords **3** with a higher yield (39%) compared with the other trifluoromethylating reagents (Table 2, entries 1, 2, and 4). Using chloride as the counterion of Umemoto's reagent further improved the yield to 54% as determined by ^{19}F NMR, which might be related to its higher water solubility (Table 2, entry 3). Tuning the irradiation wavelength (from 456 nm to 427 nm) further increases the yield of **3** to 63% (Table 2, entry 5). Interestingly, a yield of 84% was obtained when the reaction was carried out at 4 °C, which indicates that **3** is favored at lower reaction temperatures (Table 2, entry 6), likely due to the inhibition of the thermal polymerization of styrene.[55] A control experiment was run with $[Ru(bpy)_3]Cl_2$ as a photocatalyst and compared with the photocatalytic efficiency of Ru16C. Under the same reaction conditions, $[Ru(bpy)_3]Cl_2$ resulted in a 14% yield (Table 2, entry 7). Furthermore, even with the combination of 1 mol% $[Ru(bpy)_3]Cl_2$ or $Ru(bpy)_3](PF_6)$ 2 and 1 mol% CTAB, the yield is still relatively low (55% and 20%, Table 2, entries 8 and 9). This established that the ruthenium micellar system is necessary for obtaining an efficient reaction in aqueous solution. Mixing $[Ru(bpy)_3]^{2+}$ with CTAB likely sequesters the metal complex inside the micelle, limiting the number of photoactive centers in contact with the reactants and reducing the effective volume of the nanovessel. The photoactive surfactant assembling ensures a high concentration of photoactive group at the surface of the micelle and does not occupy space in the interior. Reactions using Ru10C show only 35% conversion. At 0.5 mM concentration (1 mol%), Ru10C is below the CMC and does not form micelles, supporting the importance of micelle formation for efficient catalysis. Other control experiments performed without light (Table 2, entry 10), without Ru16C (Table 2, entry 11), and without Umemoto's reagent (Table 2, entry 12) did not produce **3**, confirming the importance of light, the Umemoto's reagent, and Ru16C for the reaction to proceed. To broaden the substrate

Table 2 Optimization of hydroxytrifluoromethylation of styrene in water by ruthenium MeCS

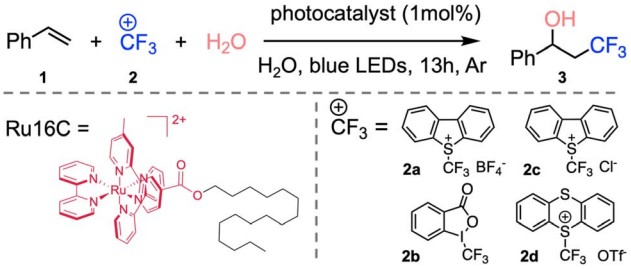

Entry[a]	CF_3 reagent	Photocatalyst	Wavelength (nm)	Yield[c] (%)
1	**2a**	Ru16C	456	39
2	**2b**	Ru16C	456	14
3	**2c**	Ru16C	456	54
4	**2d**	Ru16C	456	36
5	**2c**	Ru16C	427	63
6[b]	**2c**	Ru16C	427	84(80)[d]
7[b]	**2c**	$Ru(bpy)_3Cl_2 \cdot 6H_2O$	427	14
8[b]	**2c**	$Ru(bpy)_3Cl_2 \cdot 6H_2O$ + CTAB	427	55
9[b]	**2c**	$Ru(bpy)_3(PF_6)_2$ + CTAB	427	20
10	**2c**	Ru16C	None	0
11	**2c**	None	456	0
12	None	Ru16C	456	0

[a] Reactions were conducted on a 0.1 mmol scale using Umemoto's reagent (1.0 equiv.), styrene (1.1 equiv.), photocatalyst Ru16C or $[Ru(bpy)_3]Cl_2$ (1.0 mol%), 13 h, rt, and LED light (427 nm and 456 nm) (350 mW cm^{-2}). [b] Reactions were run in a 4 °C fridge, see the details at ESI. [c] Yields were determined from ^{19}F NMR using fluorobenzene as an NMR standard. [d] Isolated yield shown in parentheses.

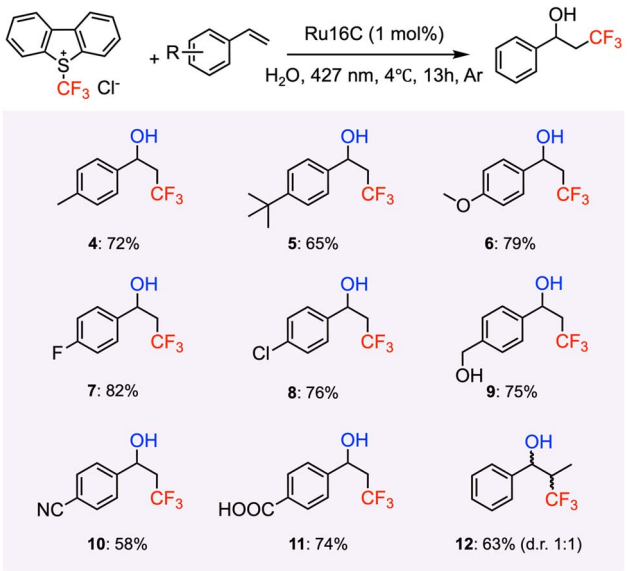

Scheme 2 Substrate scope studies of the photocatalytic hydroxytrifluoromethylation of various styrene derivatives under the default reaction condition. Yields are given as isolated products.

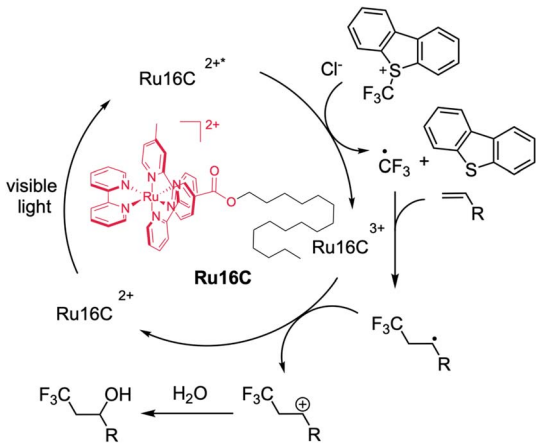

Scheme 3 Proposed mechanism for the hydorxytrifluoromethylation of styrene with ruthenium MeCSs.

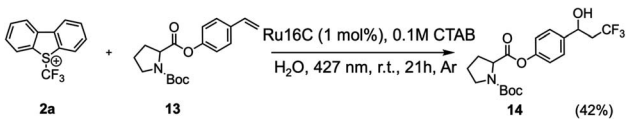

Scheme 4 Hydroxytrifluoromethylation functionalization of boc-proline derivative in water.

scope of aryl alkenes in the context of photocatalytic hydroxytrifluoromethylation employing Ru16C MeCs, various styrene derivatives were tested and summarized in Scheme 2. Styrenes bearing electron-donating groups at the para position, such as methyl (**4**), *tert*-butyl (**5**), methoxyl (**6**), and hydroxymethyl (**9**), all resulted in the corresponding products in good yields (65% to 80%). Furthermore, substrates bearing electron-withdrawing groups at the para position, including fluoro (**7**), chloro (**8**), nitrile group (**10**), and carboxylic group (**11**), were tolerated under our conditions, giving the corresponding products in moderate to good yields ranging 58% to 82%. *Trans*-*β*-methylstyrene was also examined, giving only one regioisomer (**12**) as a mixture of two diastereomers (1 : 1 d.r.) in 63% yield. To further illustrate the substrate scope and limitations of this photocatalytic hydroxytrifluoromethylation, details on unreactive and low-conversion substrates (S1–S6) have been included in the ESI.†

Mechanistically, the MeCS photocatalyst (*e.g.,* Ru16C) reaches a triplet MLCT excited state upon light absorption, which is quenched by the Umemoto's reagent to generate a CF_3 radical. The following addition of the CF_3 radical to the alkenes can result in a transient radical intermediate, which can be oxidized by the Ru(III) species, regenerating the photocatalyst and producing a carbocation intermediate. Subsequently, nucleophilic attack by water to the carbocation intermediate affords the final product (Scheme 3).[51,54] In order to confirm the formation of the CF_3 radical, one equivalent of the radical scavenger 2,2,6,6-tetramethyl-1-piperidinyloxy (TEMPO) was added to the system under the default condition. The detection of the TEMPO-CF_3 adduct on the ^{19}F NMR (Fig. S8†) corroborates the presence of CF_3 radical, which is consistent with the radical reaction pathway in Scheme 3.

To further demonstrate the synthetic capability and adaptability of MeCS photocatalyst in aqueous solution, Ru16C was used to synthesize more structurally intricate molecules derived from commercially available active pharmaceutical targets. Since research has shown that L-proline (and derivatives) exhibit anticonvulsant properties,[56] an *n*-(*tert*-butoxycarbonyl)-L-proline derivative (**13**, Scheme 4), was chosen as substrate. In our initial experiments, we found that the ruthenium MeCS concentration used in the synthesis of **3** (1 mol% of Ru16C with respect to the starting material) was insufficient to solubilize **13** effectively, leading to a solubility challenge with increasing substrate complexity. While increasing the concentration of MeCS could address the solubility problem, it will also reduce light penetration into the solution. To address this, we added 0.1 M of CTAB, which is transparent to visible light, while maintaining a relatively low photocatalyst concentration (ruthenium MeCS = 0.5 mM).[57] This system afforded product **14** with 42% isolated yield in aqueous solution.

To assess the sustainability of MeCS in the hydroxytrifloromethylation of vinylbenzene derivatives we calculated the *E* factor as described by Bu *et al.* (Scheme 5).[34] The *E* factor[58] for this photocatalytic reaction in water was calculated by

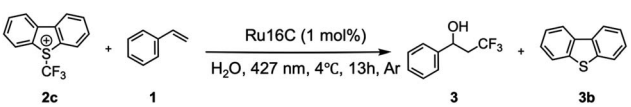

$$\text{E factor} = \frac{\text{total waste (kg)}}{\text{total product (kg)}} = 10.9$$

Scheme 5 *E* factor calculation for the trifloromethylation reaction of styrene by Ru16C MeCS.

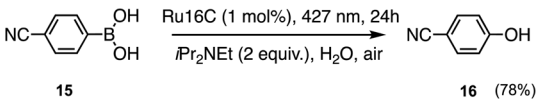

Scheme 6 Hydroxylation of aryl boronic acids by Ru16C MeCS.

considering not only the use of organic solvents for the reaction and subsequent product extraction but also the by-products generated during the transformation. This more comprehensive approach provides a more accurate measure of the process's environmental impact. The *E* factor was determined to be 10.9, which is much lower compared to traditional reactions performed in organic solvents[51] or alternative synthetic routes.[59] A detailed calculation of the *E* factor for other synthetic strategies applied to the same transformation is provided in the ESI.† Furthermore, we show that the catalyst can be recovered *via* simple mini pipette column purification (Fig. S9†) and reused in a second reaction cycle, achieving a comparable yield (82% *vs.* the initial 84%).

In addition to the hydroxytrifluoromethylation of styrene derivatives, Ru16C MeCS was found to be effective in promoting the hydroxylation of aryl boronic acids (Scheme 6).[60] This transformation was achieved under mild conditions with good yields, demonstrating the broad applicability of the catalyst. Detailed reaction conditions and product characterization are provided in the ESI.†

In conclusion, we report here a photoactive MeCS family that uses ruthenium metal complexes as a headgroup. The hydrophobicity of each MeCS was modulated by varying the length of the alkyl chain attached to the metal complex, yet all the synthesized MeCS remained highly soluble in water. The length of the aliphatic chain directly modulates the formation of the micelles, with CMC values as low as 380 μM for the ruthenium MeCS with the longest aliphatic chain. Our results show that the length of the alkyl chain has no significant effect on the absorption spectra, emission spectra, and photoluminescence lifetimes of the MeCSs. However, the quantum yield seems to increase with the length of the alkyl chain and appears to be unaffected by their incorporations in CTAB micelles. This contrasts with previous reports of double-chain ruthenium amphiphiles, where the quantum yield and lifetimes are significantly affected by their incorporation into vesicles. After evaluating the photophysical and CMC properties of each surfactant, Ru16C was selected for the photocatalytic hydroxytrifluoromethylation of aromatic olefins in aqueous solution due to its superior photophysical properties and lower CMC, with yields up to 84%. Furthermore, Ru16C can be applied in other transformation reactions in water, such as the hydroxylation of aryl boronic acids, demonstrating the versatility of MeCS. In water, the micelles' hydrophobic core serves as reaction vessels for substrates, and the hydrophilic surface functions as the photocatalyst. Our MeCS forms micelles in the range of 6 nm in diameter, which highlights the remarkable proximity effects that can occur in this micellar catalytic system. This is expected to enhance the interactions between the metal complex head group (photocatalyst) and the substrate. Finally, the recyclability of Ru16C and the use of water as a solvent significantly improve the system's sustainability.

Data availability

The data supporting this article have been included as part of the ESI.† Specific data files (such as instrument files or data spreadsheets) related to this study are available upon request from the corresponding author.

Author contributions

Conceptualization, Y. C. and A. A. M.; methodology, Y. C., A. M. Y., T. V. N., S. C. K., J. G. W., S. L. B., Y. T., and A. A. M.; investigation, Y. C., A. M. Y., T. V. N., and S. C. K.; writing – original draft, Y. C., A. M. Y., Y. T., and A. A. M.; writing – review & editing, Y. C., A. M. Y., T. V. N., S. C. K., J. G. W., S. L. B., Y. T., and A. A. M.; funding acquisition, A. A. M.; resources, J. G. W., S. L. B., Y, T., and A. A. M.; supervision, J. G. W., S. L. B., Y. T., and A. A. M.

Conflicts of interest

There are no conflicts to declare.

Acknowledgements

We acknowledge the financial support of the Welch Foundation, grant C-2152, and the Rice InterDisciplinary Excellence Award (IDEA) Award. This work was conducted in part using resources of the Shared Equipment Authority at Rice University.

References

1 K. Zeitler, *Angew. Chem., Int. Ed.*, 2009, **48**, 9785–9789.
2 T. P. Yoon, M. A. Ischay and J. Du, *Nat. Chem.*, 2010, **2**, 527–532.
3 J. M. R. Narayanam and C. R. J. Stephenson, *Chem. Soc. Rev.*, 2011, **40**, 102–113.
4 C. K. Prier, D. A. Rankic and D. W. C. MacMillan, *Chem. Rev.*, 2013, **113**, 5322–5363.
5 M. H. Shaw, J. Twilton and D. W. C. MacMillan, *J. Org. Chem.*, 2016, **81**, 6898–6926.
6 K. Teegardin, J. I. Day, J. Chan and J. Weaver, *Org. Process Res. Dev.*, 2016, **20**, 1156–1163.
7 K. L. Skubi, T. R. Blum and T. P. Yoon, *Chem. Rev.*, 2016, **116**, 10035–10074.
8 M. A. Cismesia and T. P. Yoon, *Chem. Sci.*, 2015, **6**, 5426–5434.
9 T. Koike and M. Akita, *Inorg. Chem. Front.*, 2014, **1**, 562–576.
10 T. P. Yoon, *Acc. Chem. Res.*, 2016, **49**, 2307–2315.
11 D. A. Nagib and D. W. C. MacMillan, *Nature*, 2011, **480**, 224–228.
12 D. A. Nicewicz and D. W. C. MacMillan, *Science*, 2008, **322**, 77–80.
13 C. Russo, F. Brunelli, G. C. Tron and M. Giustiniano, *J. Org. Chem.*, 2023, **88**, 6284–6293.

14 M. J. Lawrence, *Chem. Soc. Rev.*, 1994, **23**, 417.
15 S. Le Guenic, L. Chaveriat, V. Lequart, N. Joly and P. Martin, *J. Surfactants Deterg.*, 2019, **22**, 5–21.
16 T. Lorenzetto, G. Berton, F. Fabris and A. Scarso, *Catal. Sci. Technol.*, 2020, **10**, 4492–4502.
17 A. D. Smith McWilliams, S. Ergülen, M. M. Ogle, C. A. de los Reyes, M. Pasquali and A. A. Martí, *Pure Appl. Chem.*, 2020, **92**, 265–274.
18 O. Massarweh and A. S. Abushaikha, *Energy Rep.*, 2020, **6**, 3150–3178.
19 A. D. Smith McWilliams, Z. Tang, S. Ergülen, C. A. De Los Reyes, A. A. Martí and M. Pasquali, *J. Phys. Chem. B*, 2020, **124**, 4185–4192.
20 U. Umezaki, A. D. Smith McWillams, Z. Tang, Z. M. S. He, I. R. Siqueira, S. J. Corr, H. Ryu, A. B. Kolomeisky, M. Pasquali and A. A. Martí, *ACS Nano*, 2024, **18**, 2446–2454.
21 F. Mancin, P. Scrimin, P. Tecilla and U. Tonellato, *Coord. Chem. Rev.*, 2009, **253**, 2150–2165.
22 C. Schattschneider, S. Doniz Kettenmann, S. Hinojosa, J. Heinrich and N. Kulak, *Coord. Chem. Rev.*, 2019, **385**, 191–207.
23 T. Taira, *J. Oleo Sci.*, 2022, **71**, 167–175.
24 J. A. Lebrón, F. J. Ostos, M. L. Moyá, M. López-López, C. J. Carrasco and P. López-Cornejo, *Colloids Surf., B*, 2015, **135**, 817–824.
25 P. Mahato, S. Saha, S. Choudhury and A. Das, *Chem. Commun.*, 2011, **47**, 11074.
26 M. F. Ryan, R. A. Metcalfe, A. B. P. Lever and M. Haga, *J. Chem. Soc., Dalton Trans.*, 2000, 2357–2366.
27 N. Ikuta, S. Takizawa and S. Murata, *Photochem. Photobiol. Sci.*, 2014, **13**, 691–702.
28 D. Patra, A. H. Chaaban, S. Darwish, H. A. Saad, A. S. Nehme and T. H. Ghaddar, *Colloids Surf., B*, 2016, **138**, 32–40.
29 S. Nehru, S. Veeralakshmi and S. Arunachalam, *New J. Chem.*, 2017, **41**, 13830–13837.
30 S. Bhand, D. N. Lande, E. Pereira, S. P. Gejji, T. Weyhermüller, D. Chakravarty, V. G. Puranik and S. Salunke-Gawali, *Polyhedron*, 2019, **164**, 96–107.
31 I. Karakaya, *ChemistrySelect*, 2021, **6**, 11551–11556.
32 Y. Timounay, A. Pannwitz, D. M. Klein, A.-L. Biance, M. E. Hoefnagel, I. Sen, A. Cagna, M. Le Merrer and S. Bonnet, *Langmuir*, 2022, **38**, 9697–9707.
33 S. A. Bonke, G. Trezza, L. Bergamasco, H. Song, S. Rodríguez-Jiménez, L. Hammarström, E. Chiavazzo and E. Reisner, *J. Am. Chem. Soc.*, 2024, **146**, 15648–15658.
34 M. Bu, C. Cai, F. Gallou and B. H. Lipshutz, *Green Chem.*, 2018, **20**, 1233–1237.
35 E. Y. Arashiro and N. R. Demarquette, *Mater. Res.*, 1999, **2**, 23–32.
36 J. D. Berry, M. J. Neeson, R. R. Dagastine, D. Y. C. Chan and R. F. Tabor, *J. Colloid Interface Sci.*, 2015, **454**, 226–237.
37 H. Luo, C.-Y. Sun, Q. Huang, B.-Z. Peng and G.-J. Chen, *J. Colloid Interface Sci.*, 2006, **297**, 266–270.
38 X. Wang and Y. Gao, *Food Chem.*, 2018, **246**, 242–248.
39 K. Suzuki, A. Kobayashi, S. Kaneko, K. Takehira, T. Yoshihara, H. Ishida, Y. Shiina, S. Oishi and S. Tobita, *Phys. Chem. Chem. Phys.*, 2009, **11**, 9850.
40 F. Felix, J. Ferguson, H. U. Guedel and A. Ludi, *J. Am. Chem. Soc.*, 1980, **102**, 4096–4102.
41 D. W. Thompson, A. Ito and T. J. Meyer, *Pure Appl. Chem.*, 2013, **85**, 1257–1305.
42 P. Kubát and J. Mosinger, *J. Photochem. Photobiol. A: Chem.*, 1996, **96**, 93–97.
43 H. Sternlicht, G. C. Nieman and G. W. Robinson, *J. Chem. Phys.*, 1963, **38**, 1326–1335.
44 R. Knoesel, D. Markovitsi, J. Simon and G. Duportail, *J. Photochem.*, 1983, **22**, 275–283.
45 A. Sillen and Y. Engelborghs, *Photochem. Photobiol.*, 1998, **67**, 475–486.
46 M. Hansen, S. Troppmann and B. König, *Chem.–Eur. J.*, 2016, **22**, 58–72.
47 A. Pannwitz, D. M. Klein, S. Rodríguez-Jiménez, C. Casadevall, H. Song, E. Reisner, L. Hammarström and S. Bonnet, *Chem. Soc. Rev.*, 2021, **50**, 4833–4855.
48 W. Zhu, J. Wang, S. Wang, Z. Gu, J. L. Aceña, K. Izawa, H. Liu, V. A. Soloshonok and J. Fluor, *Chem*, 2014, **167**, 37–54.
49 A. S. Nair, A. K. Singh, A. Kumar, S. Kumar, S. Sukumaran, V. P. Koyiparambath, L. K. Pappachen, T. M. Rangarajan, H. Kim and B. Mathew, *Processes*, 2022, **10**, 2054.
50 Y. Ogawa, E. Tokunaga, O. Kobayashi, K. Hirai and N. Shibata, *iScience*, 2020, **23**, 101467.
51 Y. Yasu, T. Koike and M. Akita, *Angew. Chem., Int. Ed.*, 2012, **51**, 9567–9571.
52 J. W. Beatty, J. J. Douglas, K. P. Cole and C. R. J. Stephenson, *Nat. Commun.*, 2015, **6**, 7919.
53 Y. Quan, W. Shi, Y. Song, X. Jiang, C. Wang and W. Lin, *J. Am. Chem. Soc.*, 2021, **143**, 3075–3080.
54 B. K. Kundu, C. Han, P. Srivastava, S. Nagar, K. E. White, J. A. Krause, C. G. Elles and Y. Sun, *ACS Catal.*, 2023, **13**, 8119–8127.
55 W. I. Bengough and G. B. Park, *Eur. Polym. J.*, 1978, **14**, 889–894.
56 S. Sarhan and N. Seiler, *Gen. Pharmacol. Vasc. Syst.*, 1989, **20**, 53–60.
57 C.-C. Chien, S.-C. Kao, C.-J. Chen and Y.-K. Wu, *Chem. Commun.*, 2020, **56**, 15470–15472.
58 R. A. Sheldon, *Green Chem.*, 2007, **9**, 1273–1283.
59 Q. Li, W. Fan, D. Peng, B. Meng, S. Wang, R. Huang, S. Liu and S. Li, *ACS Catal.*, 2020, **10**, 4012–4018.
60 Y. Q. Zou, J. R. Chen, X. P. Liu, L. Q. Lu, R. L. Davis, K. A. Jørgensen and W. J. Xiao, *Angew. Chem., Int. Ed.*, 2012, **51**, 784–788.